NASA TECHNICAL NOTE


NASA TN D-7541

NASA TN D-7541

# AN EXPERIMENTAL INVESTIGATION OF WALL BOUNDARY-LAYER TRANSITION REYNOLDS NUMBERS IN AN EXPANSION TUBE

*by K. James Weilmuenster*

*Langley Research Center*
*Hampton, Va. 23665*




NATIONAL AERONAUTICS AND SPACE ADMINISTRATION • WASHINGTON, D. C. • MAY 1974

| 1. Report No. | 2. Government Accession No. | 3. Recipient's Catalog No. |
|---|---|---|
| NASA TN D-7541 | | |

| 4. Title and Subtitle | 5. Report Date |
|---|---|
| AN EXPERIMENTAL INVESTIGATION OF WALL BOUNDARY-LAYER TRANSITION REYNOLDS NUMBERS IN AN EXPANSION TUBE | May 1974 |
| | 6. Performing Organization Code |
| 7. Author(s) | 8. Performing Organization Report No. |
| K. James Weilmuenster | L-9337 |
| | 10. Work Unit No. |
| 9. Performing Organization Name and Address | 502-07-01-02 |
| NASA Langley Research Center<br>Hampton, Va. 23665 | 11. Contract or Grant No. |
| | 13. Type of Report and Period Covered |
| 12. Sponsoring Agency Name and Address | Technical Note |
| National Aeronautics and Space Administration<br>Washington, D.C. 20546 | 14. Sponsoring Agency Code |

15. Supplementary Notes

16. Abstract

Experimental measurements of boundary-layer transition in an expansion-tube test-gas flow are presented along with radial distributions of pitot pressure. An integral method for calculating constant Reynolds number lines for an expansion-tube flow is introduced. Comparison of experimental data and constant Reynolds number calculations has shown that for given conditions, wall boundary-layer transition occurs at a constant Reynolds number in an expansion-tube flow. Operating conditions in the expansion tube were chosen so that the effects of test-gas nonequilibrium on boundary-layer transition could be studied.

| 17. Key Words (Suggested by Author(s)) | 18. Distribution Statement |
|---|---|
| Expansion tube<br>Boundary layer<br>Transition | Unclassified – Unlimited<br><br>STAR Category 12 |

| 19. Security Classif. (of this report) | 20. Security Classif. (of this page) | 21. No. of Pages | 22. Price* |
|---|---|---|---|
| Unclassified | Unclassified | 28 | $3.25 |

*For sale by the National Technical Information Service, Springfield, Virginia 22151

# AN EXPERIMENTAL INVESTIGATION OF WALL BOUNDARY-LAYER TRANSITION REYNOLDS NUMBERS IN AN EXPANSION TUBE

By K. James Weilmuenster
Langley Research Center

## SUMMARY

Experimental measurements of boundary-layer transition in an expansion-tube test-gas flow are presented along with radial distributions of pitot pressure. An integral method for calculating constant Reynolds number lines for an expansion-tube flow is introduced. Comparison of experimental data and constant Reynolds number calculations has shown that for given conditions, wall boundary-layer transition occurs at a constant Reynolds number in an expansion-tube flow. Operating conditions in the expansion tube were chosen so that the effects of test-gas nonequilibrium on boundary-layer transition could be studied.

## INTRODUCTION

The development of the expansion tube as a hypervelocity facility has entailed the study of several effects which cause the resulting flow parameters to differ from their ideal values. One such phenomenon, reported in reference 1, is that under certain operating conditions the test-gas flow experiences a rather sudden drop or dip in pitot pressure. It was at first thought that this dip in pitot pressure could be attributed to the secondary diaphragm since the energy loss from the flow was of the same order as that required to rupture the secondary diaphragm. However, parametric studies involving the strength and mass of the secondary diaphragm show no effect on the dip. Mixing of the acceleration and test gases offered another possible explanation for the pitot-pressure drop.

Mirels' (ref. 2) theory of shock attenuation shows that in order to maintain a mass balance, a great deal of the shocked acceleration gas is fed into the boundary layer which lies between the tube wall and the test gas. Any mixing of the shocked acceleration gas and the test gas would produce pitot pressures which are lower than those predicted for the test gas. Thus, the reduction in the pitot pressure might indicate the diffusion of acceleration gas contained in the wall boundary layer into the free stream. Extensive

tests to determine whether the test gas was indeed contaminated by the shocked acceleration gas were negative.

As suggested by the authors of reference 1, the transition from a laminar boundary layer to a turbulent boundary layer on the tube wall in the test gas along with the more rapid boundary-layer growth and subsequent closure is proposed as an explanation for the drop in pitot pressure. Thus, the ability to track and predict transition would be important as a parameter in determining expansion-tube test time and operating conditions. This paper is concerned with the experimental tracking of wall boundary-layer transition through the expansion tube and the calculation of transition Reynolds numbers. Data for this study were taken in the 9.525-cm-diameter Langley pilot model expansion tube which is described in reference 1.

## SYMBOLS

Primary measurements have been made in U.S. Customary Units and converted to SI Units.

$a$ speed of sound, meters/second

$b$ integrated Reynolds number parameter defined by equation (2)

$p$ pressure, newtons/meter$^2$

$p_t$ pitot pressure, newtons/meter$^2$

$R$ Reynolds number

$R_f$ general integrated Reynolds number through the expansion fan

$R_{f,o}$ integrated Reynolds number of the reference particle due to traversing the expansion fan

$R_{l,i}$ unit Reynolds number in region $i$

$R_t$ total integrated Reynolds number

$R_{②,fan} = R_{②} + R_f$

$r$ tube radius

$S_i$ shock propagating into region i

t time, seconds

U velocity, meters/second

x distance, meters

y distance measured from tube wall

Subscripts:

$\ell$ center line

ent expansion-fan entrance conditions

ex expansion-fan exit conditions

f regions of flow affected by an unsteady expansion

i regions in flow at different thermodynamic states denoted by ① . . . ⑳

o reference conditions

p particle property

tr reference to transition

Primes denote coordinates referenced to apex of centered expansion fan.

## EXPANSION-TUBE OPERATION

In the operating cycle of an expansion tube, a very short duration steady flow is produced at hypersonic conditions. An idealized schematic of the expansion-tube flow cycle is shown in figure 1. The principles of operation are discussed in detail in reference 3.

Briefly, the facility consists of a high-pressure driver section which is charged with either hydrogen or helium, an intermediate section which is charged with a test gas of interest, and an acceleration section which is normally charged with helium at a

low density. A heavy steel diaphragm separates the driver and intermediate sections and a thin plastic diaphragm separates the intermediate and acceleration sections. A shock-tube flow is initiated when the primary diaphragm is ruptured. The incident shock then ruptures the secondary diaphragm and induces another shock-tube-like flow, where the driven gas of the first flow becomes the driver gas for the second flow. Gas processed by the shock in the acceleration section is separated by an interface from the test gas (region ⑤). A history of the processed test gas is indicated by a particle path originating in the intermediate section. This path represents a picture of the ideal, inviscid expansion-tube cycle. The inclusion of viscous and real-gas effects can significantly alter the previous description primarily through shock attenuation as described by Mirels (refs. 2 and 4) and nonequilibrium effects reported by Haggard (ref. 5).

The experimental data that are presented in this paper were taken from a series of runs in the Langley pilot model expansion tube. The driver, test, and acceleration gases as well as the initial pressure in the driver and acceleration sections of the expansion tube remained the same throughout the tests. The driver gas was $H_2$ at a pressure of 8.9 $MN/m^2$ and the acceleration gas was He at a pressure of 0.27 $kN/m^2$. The only parameter varied was the initial pressure of the test gas which was air. This change in pressure had the effect of causing a significant change in the unit Reynolds number in regions ② and ⑤ although $U_{⑤}$ only varied from 3698 m/sec to 4622 m/sec.

Flow parameters measured at the test section were made at different axial locations downstream of the second diaphragm by moving the diaphragm station relative to the fixed test section.

## PITOT-PRESSURE DIP PHENOMENON

Dips in the pitot pressure in region ⑤ were first noted in reference 1 on center-line pitot-pressure records taken in the test section as illustrated by the lower oscillogram trace in figure 2.

The small initial pressure rise is caused by the arrival of the shock $S_{⑩}$, followed by the region ⑳ (acceleration gas), while the second rise is caused by the arrival of the interface, with the subsequent region ⑤ (test gas) following. The pitot-pressure level in region ⑤ should persist for approximately 200 $\mu$sec at a constant level and then rise as the unsteady expansion arrives at the test section. As seen in figure 2, the region ⑤ pitot pressure remains constant for approximately 40 $\mu$sec, drops sharply, and then begins to rise again. The upper trace in figure 2 is the wall static pressure taken at a station 26.5 cm upstream of the test section. When plotted on an x,t diagram, the high-frequency pressure fluctuations seen on the wall static pressure correlate well with the initiation of the dip in pitot pressure measured on the center line.

The high-frequency pressure fluctuations in the wall static pressure are indicative of the situation found in a turbulent boundary layer. However, as shown in figure 3, expansion-tube operating conditions have been found so that there is no apparent dip in the center-line pitot pressure whereas the wall static pressure still indicated the onset of the high-frequency pressure changes. Thin-film heat-transfer gages were placed in the tube wall to be used as further indication of transition. There was a good correlation between the time of onset of wall pressure fluctuations in figure 3 and the time of boundary-layer transition as indicated on wall-temperature records in figure 4. The time at which transition occurs in figures 3 and 4 is measured relative to the time of arrival of the incident shock as noted in the respective figures. Further investigation showed, as indicated in figure 5, that at the same conditions as the data presented in figures 3 and 4, pitot-pressure samples taken at one-half the tube radius above and below the center line indicated a presence of the pitot-pressure dip, an indication that the disturbance causing the dip moved from the tube walls toward the center line. Also, an order-of-magnitude reduction in the region unit Reynolds number used for the data shown in figures 3 to 5 was found to eliminate pitot-pressure dip as shown in figure 6. The exact nature of the disturbance seen on all the records in figure 6, approximately 800 $\mu$sec after the arrival of the incident shock, is not clear. It could be related to boundary-layer transition or to upstream moving waves associated with the normal operating cycle of the expansion tube. Similar data were reported by Jones and Moore. (See ref. 1.)

Since the pitot-pressure dip moves from the tube walls to the center line and appears to be associated with indications of boundary-layer transition, it was believed that the pitot-pressure dip is triggered by the arrival of the outer edge of a rapidly growing turbulent boundary layer at the radial location of a pitot-pressure probe because of the reduction of total pressure and velocity in the boundary layer. The same phenomenon would occur if the boundary layer were laminar since, for a given tube diameter, boundary-layer closure would occur after a sufficiently long time. However, this condition is unlikely to occur because of the short times involved and the character of the boundary layer in an expansion-tube-like flow as described by Trimpi and Cohen. (See ref. 6.)

In an attempt to understand the dip phenomenon better, a five-probe pitot-pressure rake was designed and tested in the Langley pilot model expansion tube. The rake was designed so that the pressure transducers were located near the leading edge of the rake; thus, the response time of the probe was minimized. This rake sampled the pitot pressure on the center line and in four equal increments to a position $y/r = 0.275$. Thus, a radial sampling of the expansion-tube flow was obtained. Some of the results from these tests are shown in figures 7 to 9 for three different axial locations. Because the flow can be sampled at only one axial location per run, the data for each axial location

correspond to a different run. Efforts were made to maintain the same flow properties for each test run. Each of the pitot-pressure profiles is normalized with respect to the center-line pitot pressure. The oscillations in the pitot pressure have been eliminated, and the resulting smoothed curves have been plotted at the top of each figure.

Several difficulties were encountered in the acquisition of the pitot-pressure data, the most significant being the acceleration sensitivity of the pressure transducers used in the rake. This acceleration sensitivity caused an estimated 20- to 30-percent uncertainty in the data. Therefore, the data as shown in figures 7 to 9 are only intended to show possible trends in the development of the expansion-tube test-gas flow. It may be noted that the trend is for the dip to occur earlier in time relative to the interface as the point of data sampling is moved downstream of the secondary diaphragm, and for the wall boundary layer to grow at a more rapid rate in the vicinity of the dip. Also, the pitot pressure indicates that the tube is almost filled by the boundary layer when the dip occurs; this condition might explain why the effects of transition are seen on the center line such a short time after transition is detected at the wall.

The following sections of the paper are based on the hypothesis that the wall static-pressure and heat-transfer records provide adequate definition of wall boundary-layer transition. Next, an effort will be made to determine the proper transition Reynolds number to use and to determine whether transition occurs at a constant Reynolds number or is a function of unit Reynolds number.

## RESULTS AND DISCUSSION

In a flow as complex as that found in the expansion tube, an a priori analysis to determine transition Reynolds numbers would be, at best, exceedingly difficult and no attempt will be made here to carry over steady-flow criteria to unsteady flow. As an alternative, a plausible method of calculating the pertinent Reynolds number for the experimental data is presented.

When working with boundary-layer transition in a shock tube, Hartunian et al. (ref. 7) based the transition Reynolds number on distance a particle travels in the shocked gas before it reaches the transition point, which is equivalent to the path of the transition point being parallel to the path of the shock. Although there was some scatter in the experimental data, the use of this Reynolds number correlated his data very well. One might then expect the locus of points representing transition in the expansion-tube test gas to be at some fixed or nearly fixed distance from the contact surface. A plot of experimental transition points on an $x,t$ diagram is shown in figure 10. As can be seen, the data hardly satisfy the previous assumption. The path of transition moves toward the contact surface or interface and eventually intersects it.

If a return is made to the idea of basing the Reynolds number on the distance a particle has traveled since being set in motion, the form of the Reynolds number to be used must be determined since the particle must traverse regions of variable unit Reynolds number. Since the test gas is first set in motion by the shock $S_{①}$ and is then processed by an unsteady expansion, no uniform axial free-stream properties are available with which to form a Reynolds number. The concept of an integrated Reynolds number has been used in boundary-layer transition studies on cones (Nagamatsu and Sheer (ref. 8)) and on nozzle walls. A total integrated Reynolds number is defined as

$$R_t = \sum R_i$$

where

$$R_i = \int_{x_{p,i}} R_{l,i}(x)\, dx$$

The total Reynolds number is based on the Reynolds number accumulated by a particle (as shown in fig. 11) as it traverses the region ② (a region of constant free-stream properties), the unsteady expansion (a region of varying free-stream properties), and region ⑤ (a region of constant free-stream properties). Thus, $R_t$ takes the form

$$R_t = R_{l,②} \int_{x_{p,②}} dx + \int_{x_{p,f}}^{x_{p,⑤}} R_l(x)\, dx + R_{l,⑤} \int_{x_{p,⑤}} dx$$

Determination of the integrated Reynolds numbers in regions ② and ⑤ is straightforward. The procedure for carrying out the integration over the unsteady expansion fan was accomplished as follows. By use of the flow properties in region ② as the initial conditions, thermodynamic properties based on frozen or equilibrium air were determined through the expansion fan for 30.48 m/sec increments in the velocity until the value of $U_{⑤}$ was reached. Since the expansion fan is time-similar (conical) with respect to its origin, it is convenient to locate a new $t',x'$ coordinate system, as shown in figure 11, with the origin at the apex of the centered expansion fan. Also, because the flow is conical, it is only necessary to determine one value of the integrated Reynolds number through the fan since the Reynolds number of any other particle traversing the fan can be scaled to that calculated value. Therefore, an arbitrary reference time at which a particle enters the fan $t'_{o,ent}$ is picked and $x'_{o,ent}$ is determined from

$$x'_{o,ent} = t'_{o,ent}\left(U_{②} - a_{②}\right)$$

A Runge-Kutta type of integration is then carried out so that the position of the particle on each of the incremental U - a characteristics is known. This integration then gives the thermodynamic state of the particle as a function of its position and the final integration,

$$R = \int_{x_{p,f}} R_l(x)\, dx$$

is done by Simpson's rule. Thus, the integrated Reynolds number of any particle traversing the fan can be characterized by this reference Reynolds number $(R_{f,o})$, the reference times $(t'_{o,ent}$ and $t'_{o,ex})$ at which the reference particle enters and exits the expansion fan, and the time $(t'_{ent})$ at which the particle of interest enters the fan.

The integrated Reynolds number in region ② and expansion fan can be combined to give an analytic expression for the integrated Reynolds number at the trailing edge of the expansion fan. By reference to figure 11, the path of the shock $S_①$ is

$$t' = \frac{x'}{U_{S,①}} \tag{1}$$

and that of the particle in region ② is

$$t' = \frac{x'}{U_②} + b \tag{2a}$$

Also,

$$b_o = t'_{o,ent} - \frac{x'_{o,ent}}{U_②}$$

For some arbitrary value of $t'_{ent}$,

$$b = \frac{t'_{ent}}{t'_{o,ent}}\, b_o$$

and equation (2) becomes

$$t' = \frac{x'}{U_②} + \frac{t'_{ent}}{t'_{o,ent}}\, b_o \tag{2b}$$

Equations (1) and (2b) are solved simultaneously to give the point at which the particle was set in motion

$$x'_p = \frac{\left(\frac{t'_{ent}}{t'_{o,ent}}\right) b_o}{\frac{1}{U_{S,①}} - \frac{1}{U_②}} \tag{3}$$

The point at which the particle enters the fan is

$$x'_{p,ent} = t'_{ent}\left(U_② - a_②\right) \tag{4}$$

Subtracting equation (3) from equation (4) gives $\Delta x_{p,②}$, the total distance that the particle has traveled in region ②.

The integrated Reynolds number in region ② is simply

$$R_② = R_{l,②}\, \Delta x_{p,②} \tag{5}$$

Since the flow in the expansion fan is conical, the integrated Reynolds number through the fan scales is

$$\frac{R_f}{R_{f,o}} = \frac{x'_{ex} - x'_{ent}}{x'_{o,ex} - x'_{o,ent}} \tag{6}$$

where

$$x'_{ex} = \left(U_⑤ - a_⑤\right) \frac{t'_{ent}}{t'_{o,ent}}\, t'_{o,ex}$$

and

$$x'_{ent} = \left(U_② - a_②\right) t'_{ent}$$

so that

$$R_f = \left[\left(U_⑤ - a_⑤\right) \frac{t'_{o,ex}}{t'_{o,ent}} - \left(U_② - a_②\right)\right] t'_{ent}\, \frac{R_{f,o}}{x'_{o,ex} - x'_{o,ent}} \tag{7}$$

Therefore, the total integrated Reynolds number to the point at which the particle exits the expansion fan is

$$R_{②,fan} = \left\{ \left[ \left(U_{⑤} - a_{⑤}\right) \frac{t'_{o,ex}}{t'_{o,ent}} - \left(U_{②} - a_{②}\right) \right] \frac{R_{f,o}}{x'_{o,ex} - x'_{o,ent}} \right.$$

$$\left. + \left[ \left(U_{②} - a_{②}\right) - \frac{b_o}{t'_{o,ent}} \left( \frac{1}{U_{S,①}} - \frac{1}{U_{②}} \right)^{-1} \right] R_{l,②} \right\} t'_{ent} \tag{8}$$

and that point is given by

$$t'_{ex} = \frac{t'_{o,ex}}{t'_{o,ent}} t'_{ent}$$

and

$$x'_{ex} = \left(U_{⑤} - a_{⑤}\right) t'_{ex} \tag{9}$$

Since lines of constant Reynolds number will be of interest, they may be plotted by inverting equation (8) and solving for $t'_{ent}$ while holding $R_t$ constant and marching through the expansion fan in increments of velocity so that $U_i - a_i$ represents the termination of the expansion fan. Then

$$t'_{ent,i} = \frac{R_t}{\left[ \left(U_i - a_i\right) \left( \frac{t'_{o,ex,i}}{t'_{o,ent}} \right) - \left(U_{②} - a_{②}\right) \right] \frac{R_{f,o}}{x'_{o,ex} - x'_{o,ent}} + \left[ \left(U_{②} - a_{②}\right) - \frac{b_o}{t'_{o,ent} \left( \frac{1}{U_{S,①}} - \frac{1}{U_{②}} \right)} \right] R_{l,②}} \tag{10}$$

and

$$\left.\begin{aligned} t'_{ex,i} &= \left( \frac{t'_{o,ex,i}}{t'_{o,ent}} \right) t'_{ent,i} \\ x_{ex,i} &= \left(U_i - a_i\right) t'_{ex,i} \end{aligned}\right\} \tag{11}$$

Constant Reynolds numbers in region ⑤ will be on the line

$$x' = x'_{ex} + \left( \frac{R_t - R_{②,fan}}{R_{l,⑤}} \right) \qquad \left(R_t > R_{②,fan}\right) \tag{12}$$

and

$$t' = t'_{ex} + \frac{x' - x'_{ex}}{U_{⑤}} \tag{13}$$

This procedure was carried out for the same conditions as used for figure 10. A series of constant Reynolds number curves were generated and the curve which seemed to best fit the data was $R_{tr} = 40 \times 10^6$ as shown in figure 12. There is good agreement at the end points, but there is considerable difference between the data and the calculated Reynolds number about 9 meters downstream of the diaphragm. Haggard (ref. 5) has shown that for a range of operating conditions which includes this particular example, the early part of the flow processed by the expansion lags the local equilibrium state. Succeeding sections of the flow begin to approach, but do not reach, the equilibrium state. Consequently, in an attempt to estimate the effects of nonequilibrium flow on $R_t$, lines of constant integrated Reynolds number were generated by assuming that the flow was frozen at the region ② condition. The Reynolds number $40 \times 10^6$ curve for the frozen case is plotted along with the previous data in figure 13. It may be assumed that the cases for relaxing flow lie between these two limits. Here, as with subsequent plots involving values calculated from the frozen state, only the equilibrium head and tail of the expansion fan are plotted, although there are small differences between the equilibrium and frozen characteristics. The data points lie first on the curve determined by assuming frozen flow, and then shift to the curve representing the same total Reynolds number, but were calculated under the assumption that the flow is in equilibrium.

To check the validity of the frozen to equilibrium transition and to check on unit Reynolds number effect, two other cases were run. The first used a value of $p_{①}$ that would produce a flow closely approximating the totally frozen flow. The results of this case are shown in figure 14. There is excellent agreement between a frozen transition Reynolds number of $10 \times 10^6$ and the experimental data. A second case, shown in figure 15, used a value of $p_{①}$ which will approximate the flow in equilibrium. Again, the data points agree very well with a value of $R_{tr}$ of $40 \times 10^6$. However, since for this case there is little difference in the equilibrium and frozen states of the gas, it is difficult to tell whether the flow is relaxing.

For each run made, wall boundary-layer transition along the tube was found to occur at a single transition Reynolds number which was calculated by use of an integral technique. The integrated Reynolds number works equally well when the flow is in either the near-equilibrium or near-frozen flow regimes as well as when the flow transits between these two limiting cases. Thus, it is only necessary to determine one experimental transition data point in order to calculate the location of transition throughout the length of the expansion-tube acceleration chamber provided that point is determined before transition reaches the interface.

In all three cases shown, the constant Reynolds number curves representing transition intersect the path of the interface and terminate at that point. This condition is due to a discontinuity in $R_l$ at the interface. There was no experimental evidence to indicate that the point of transition moved across the interface into the acceleration gas. In fact, the data show (fig. 15) that once the point of transition reached the interface, it continued to move with the interface.

There are two possible explanations for this behavior of the transition point. First, had it been possible to make measurements much further downstream, the transition point might have moved across the interface. Because $R_{l,⑤} >> R_{l,⑳}$, it would take a particle initially at rest and just downstream of the secondary diaphragm much longer to reach the transition Reynolds number than it would a particle just upstream of the diaphragm. Second, the structure of the wall boundary layers in regions ⑳ and ⑤ is fundamentally different, one being made up of hot acceleration gas and the other consisting of an upper layer of cool test gas and a lower layer of hot acceleration gas. It is not realistic to expect one Reynolds number to determine transition in these two different regions, nor would one expect the point of transition to move continuously between boundary layers having such radically different structure.

Since the path of transition does eventually intersect the interface, transition limits the available test time in an expansion tube, the maximum test time available occurring at the point where transition crosses the tail of the unsteady expansion.

Some care must be taken when relating these data to the flow in similar facilities. The Langley pilot model expansion tube had unmachined, extruded tube walls which might affect the location of transition when compared with transition in a facility where care had been taken to maintain smooth tube walls. Also, the disruptive effects of transition on the free-stream flow, namely, the pitot-pressure dip, are related to the ratio of wall boundary-layer thickness to the tube radius. Consequently, if the conditions presented here were used in a tube having a much larger diameter than the tube used in this study, one would expect to see the available test time increase for the same running conditions because of the increased time required for the boundary layer to fill the tube.

The effect of unit Reynolds number on the transition Reynolds number is shown in figure 16, where $R_{tr}$ is plotted against $R_{l,②}$. There is, as can be seen, some variation; however, the evidence is inconclusive because of the limited data available. It is of interest to note that although the spread in $R_{tr}$ is relatively small $(10 \times 10^6$ to $40 \times 10^6)$, these values bracket a very large area on the x,t diagram as illustrated in figure 14.

## CONCLUDING REMARKS

Wall boundary-layer transition has been measured experimentally in the Langley pilot model expansion tube. It has been shown that boundary-layer transition occurs along the length of the expansion-tube acceleration chamber at a constant transition Reynolds number up to the time at which the path of transition intersects the interface. The integral method of calculating the transition Reynolds number worked equally well for equilibrium flow, frozen flow, and flow in transition between these two limiting cases. Although transition criteria established in this paper may not be applicable to similar facilities, it has been established that if an experimental transition data point is given, the integral method developed in this paper will predict the location of transition along the tube.

Transition of the wall boundary layer was found to be a factor in limiting the available test time in the expansion tube under certain operating conditions. However, it would be inappropriate to apply the present results directly to tubes of different diameter and wall roughness.

Langley Research Center,
National Aeronautics and Space Administration,
Hampton, Va., February 5, 1974.

## REFERENCES


1. Jones, Jim J.; and Moore, John A.: Exploratory Study of Performance of the Langley Pilot Model Expansion Tube With a Hydrogen Driver. NASA TN D-3421, 1966.

2. Mirels, Harold: Test Time in Low-Pressure Shock Tubes. Phys. Fluids, vol. 6, no. 9, Sept. 1963, pp. 1201-1214.

3. Trimpi, Robert L.: A Preliminary Theoretical Study of the Expansion Tube, a New Device for Producing High-Enthalpy Short-Duration Hypersonic Gas Flows. NASA TR R-133, 1962.

4. Mirels, Harold: Shock Tube Test Time Limitation Due to Turbulent-Wall Boundary Layer. AIAA J., vol. 2, no. 1, Jan. 1964, pp. 84-93.

5. Haggard, Kenneth V.: Free-Stream Temperature, Density, and Pressure Measurements in an Expansion Tube Flow. NASA TN D-7273, 1973.

6. Trimpi, Robert L.; and Cohen, Nathaniel B.: An Integral Solution to the Flat-Plate Laminar Boundary-Layer Flow Existing Inside and After Expansion Waves and After Shock Waves Moving Into Quiescent Fluid With Particular Application to the Complete Shock-Tube Flow. NACA TN 3944, 1957.

7. Hartunian, R. A.; Russo, A. L.; and Marrone, P. V.: Boundary-Layer Transition and Heat Transfer in Shock Tubes. J. Aerosp. Sci., vol. 27, no. 8, Aug. 1960, pp. 587-594.

8. Nagamatsu, H. T.; and Sheer, R. E., Jr.: Boundary-Layer Transition on a $10^{\circ}$ Cone in Hypersonic Flows. AIAA J., vol. 3, no. 11, Nov. 1965, pp. 2054-2061.

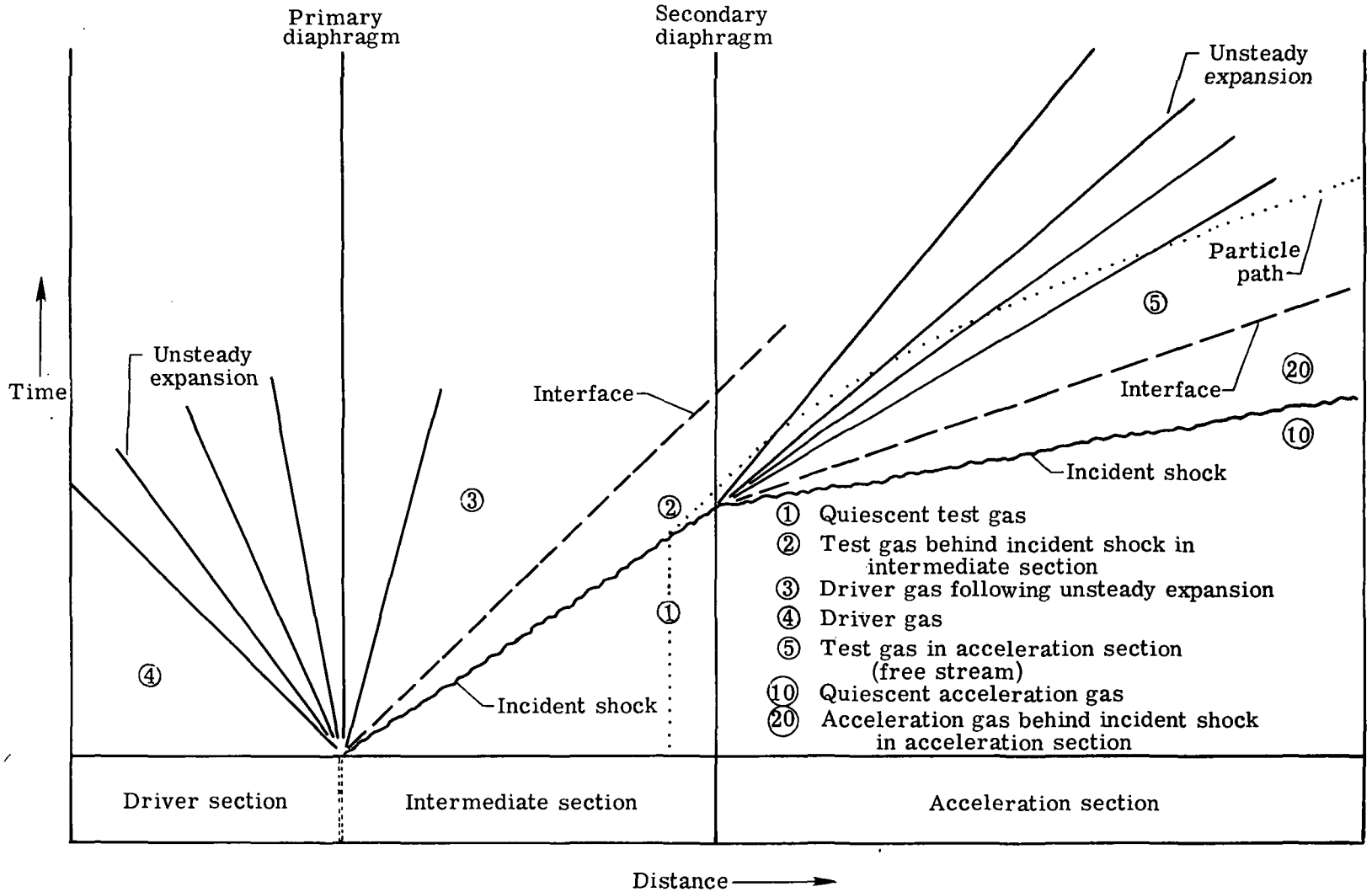


Figure 1.- Schematic diagram of expansion-tube flow cycle.

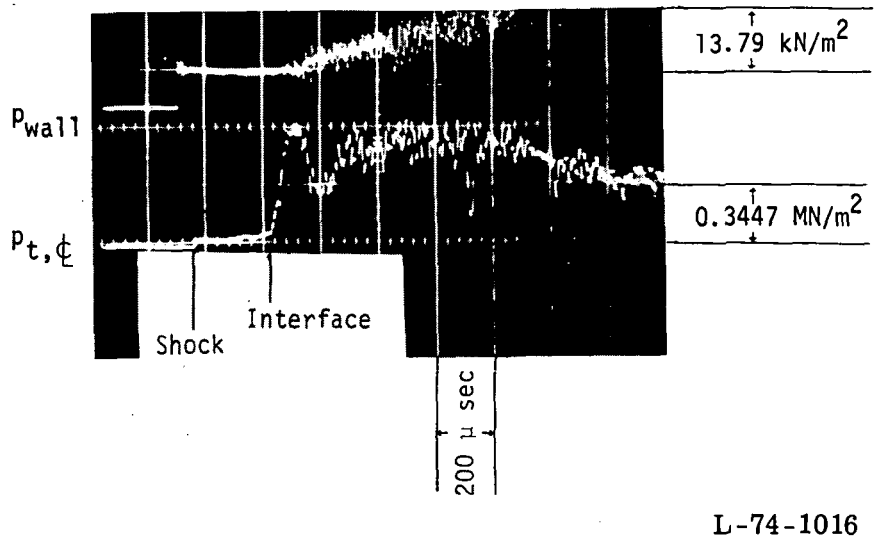


Figure 2.- Center-line pitot pressure and wall static pressure.

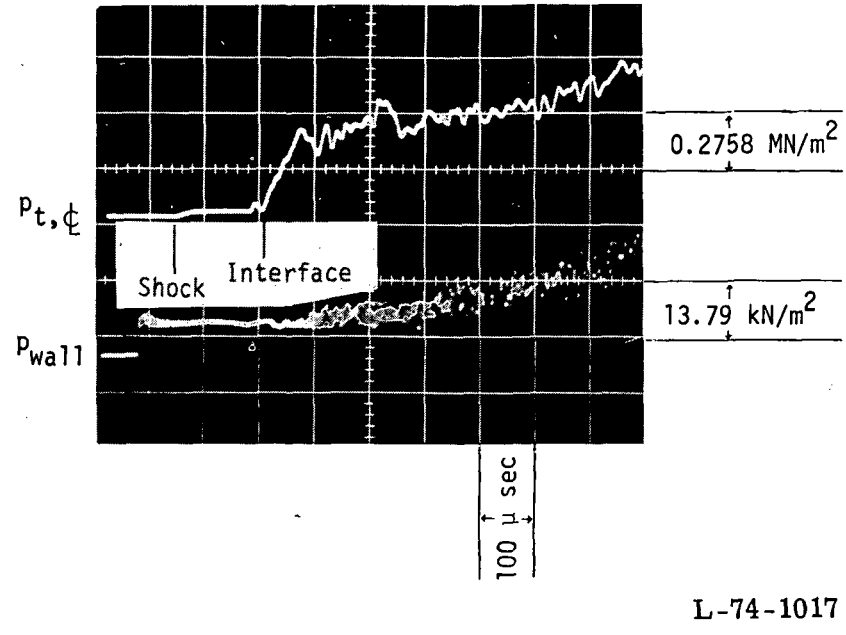


Figure 3.- Center-line pitot pressure and wall static pressure.

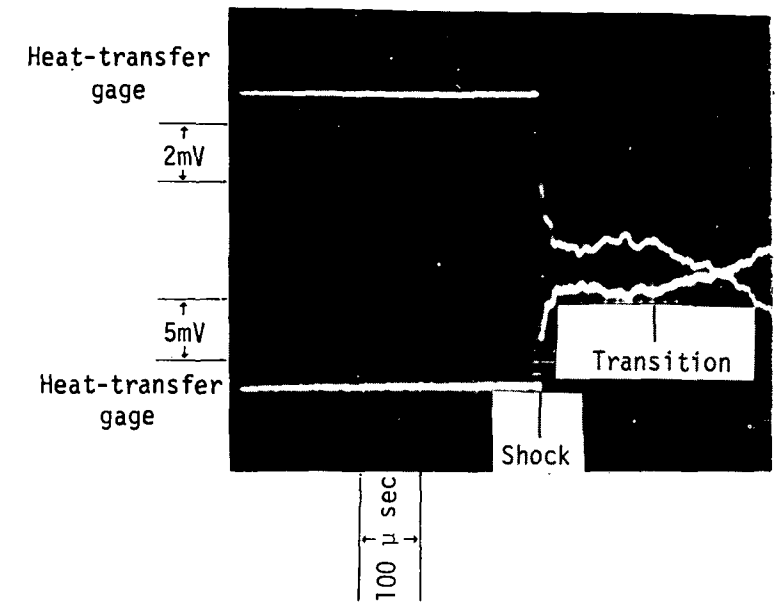


L-74-1018

Figure 4.- Wall-temperature records.

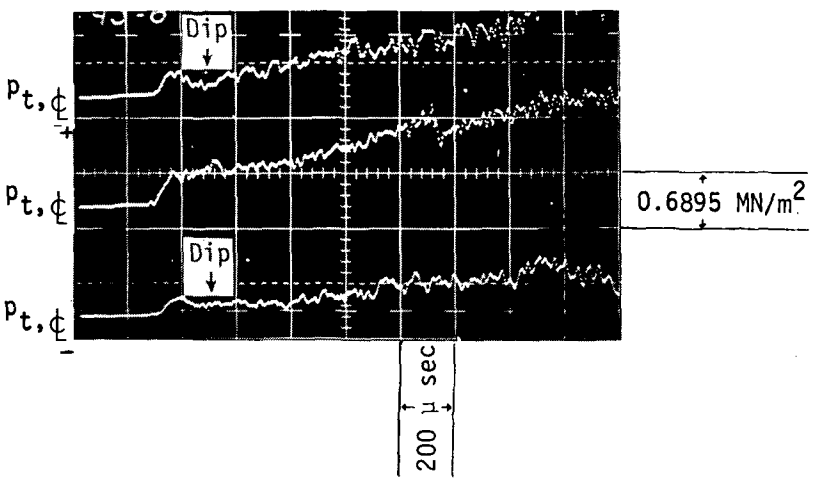


L-74-1019

Figure 5.- Radial distribution of pitot pressure.

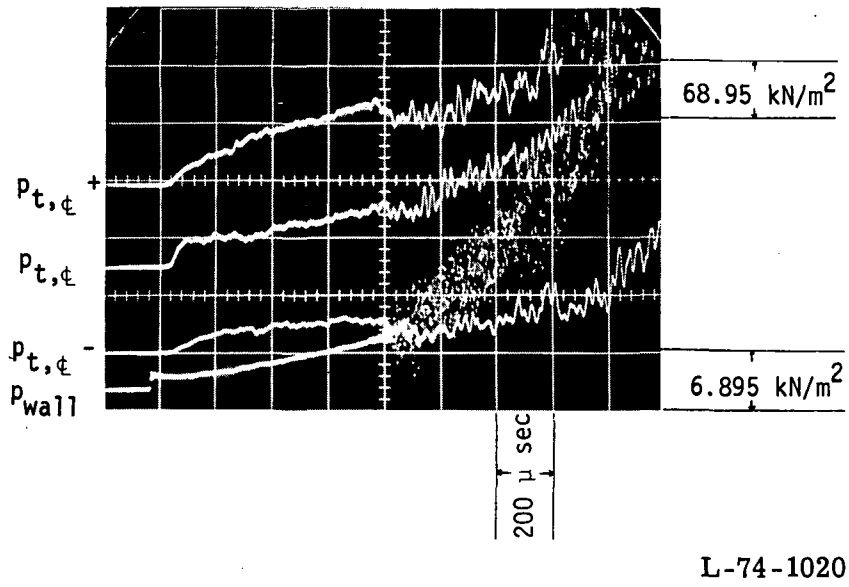


Figure 6.- Wall static pressure and radial distribution of pitot pressure.

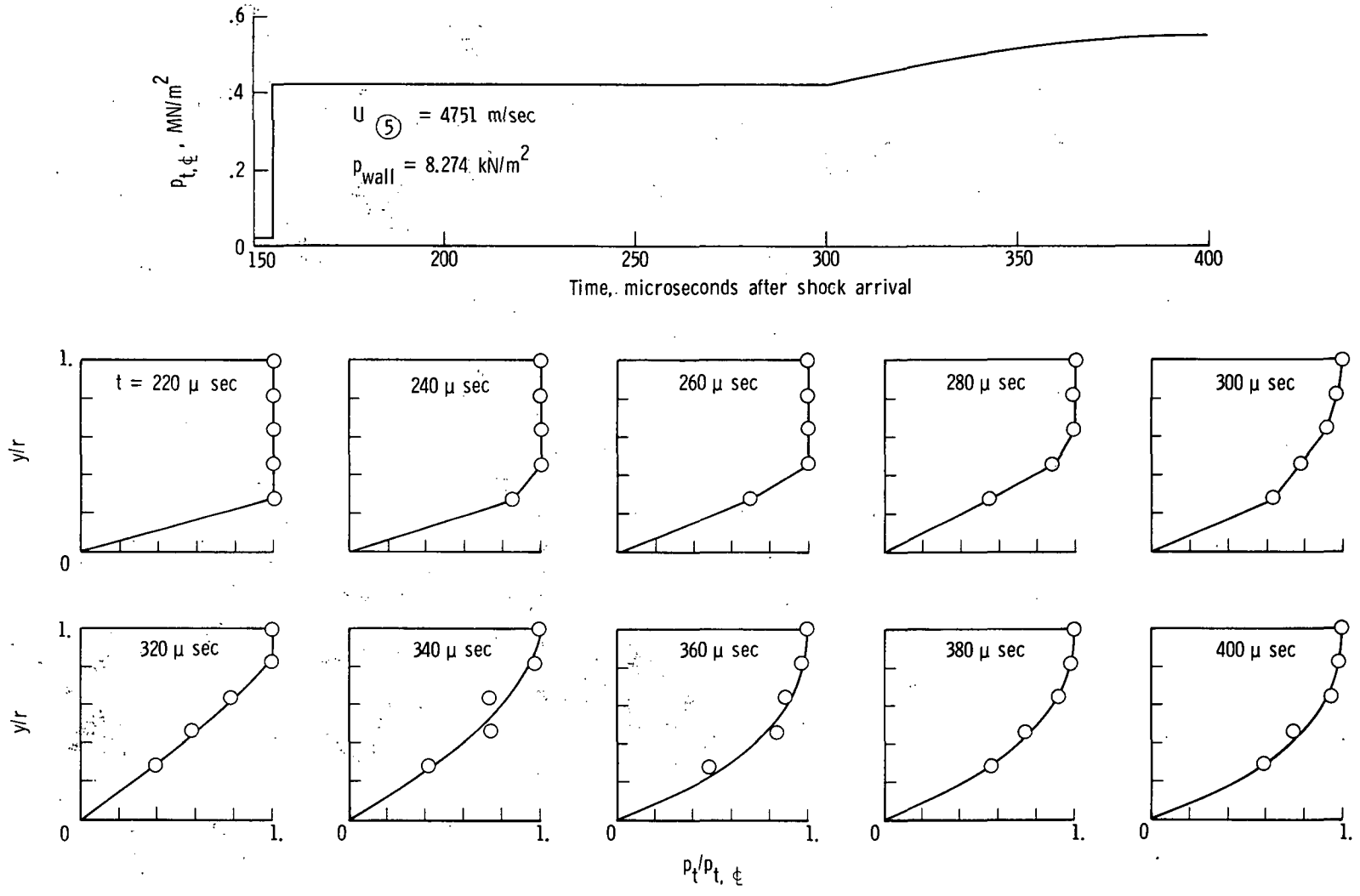


Figure 7.- Center-line pitot pressure and pitot-pressure profiles at x = 6.035 meters downstream of secondary diaphragm.

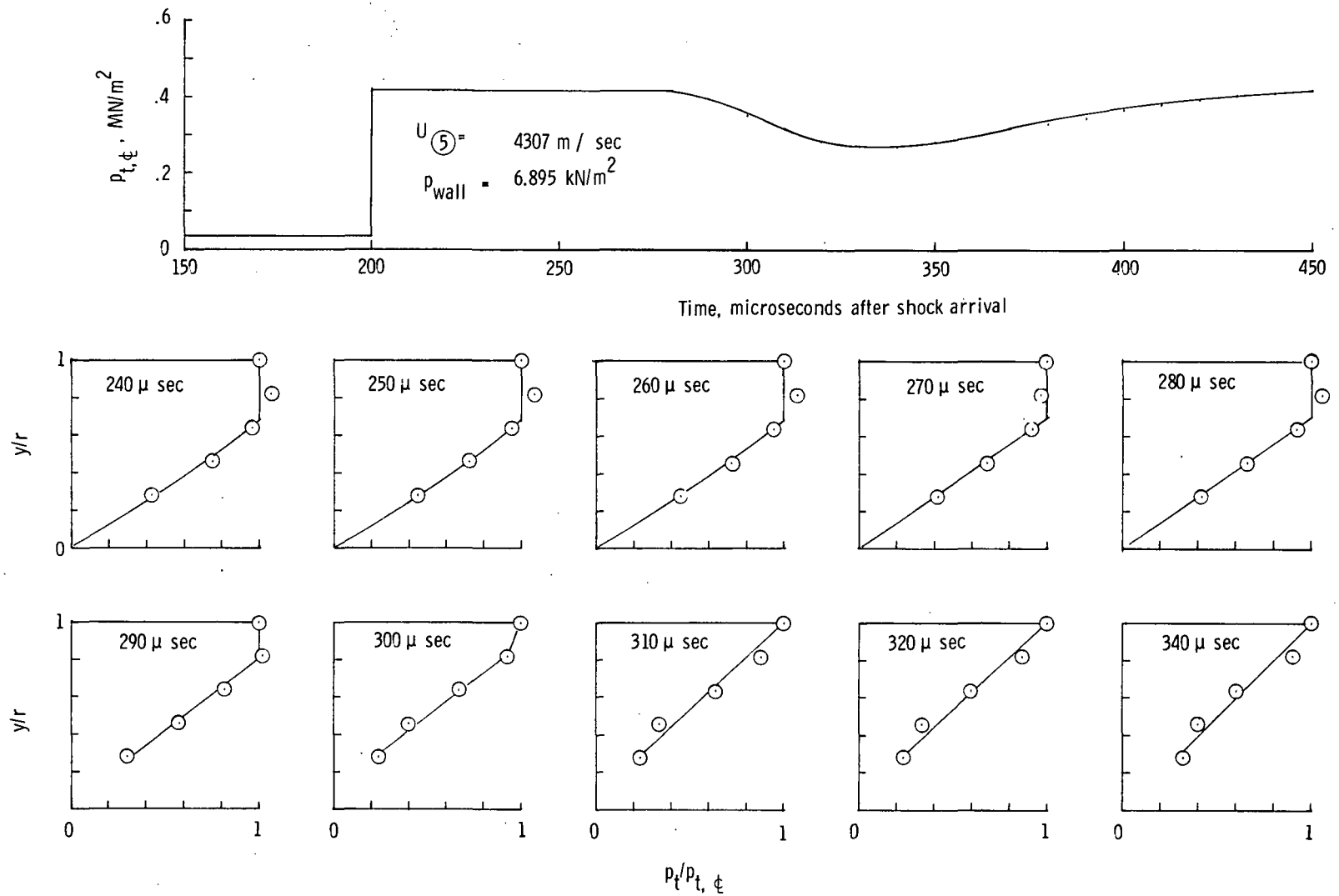


Figure 8.- Center-line pitot pressure and pitot-pressure profiles at x = 9.692 meters downstream of secondary diaphragm.

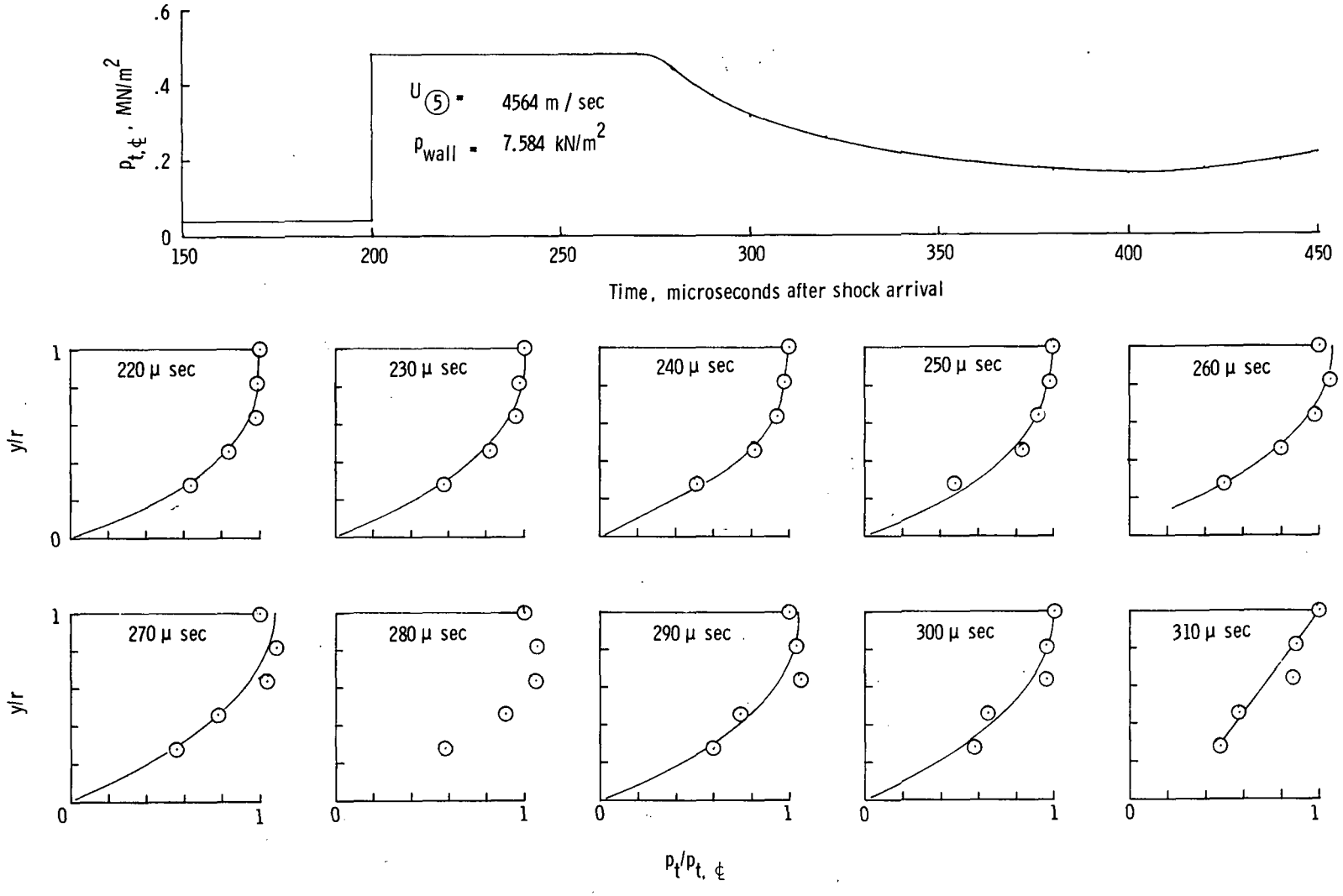


Figure 9.- Center-line pitot pressure and pitot-pressure profiles at x = 12.983 meters downstream of secondary diaphragm.

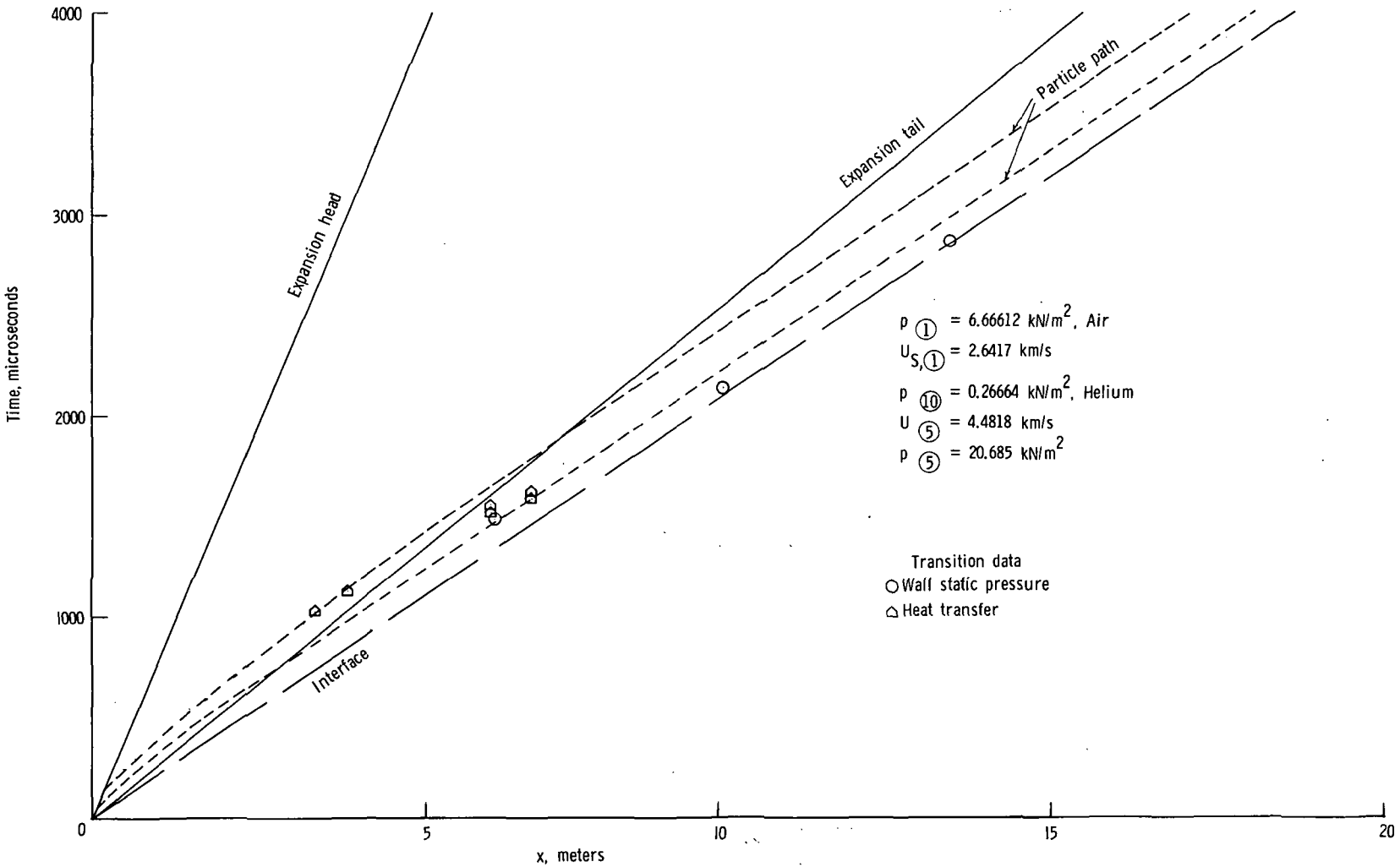


Figure 10.- Transition data as a function of particle path.

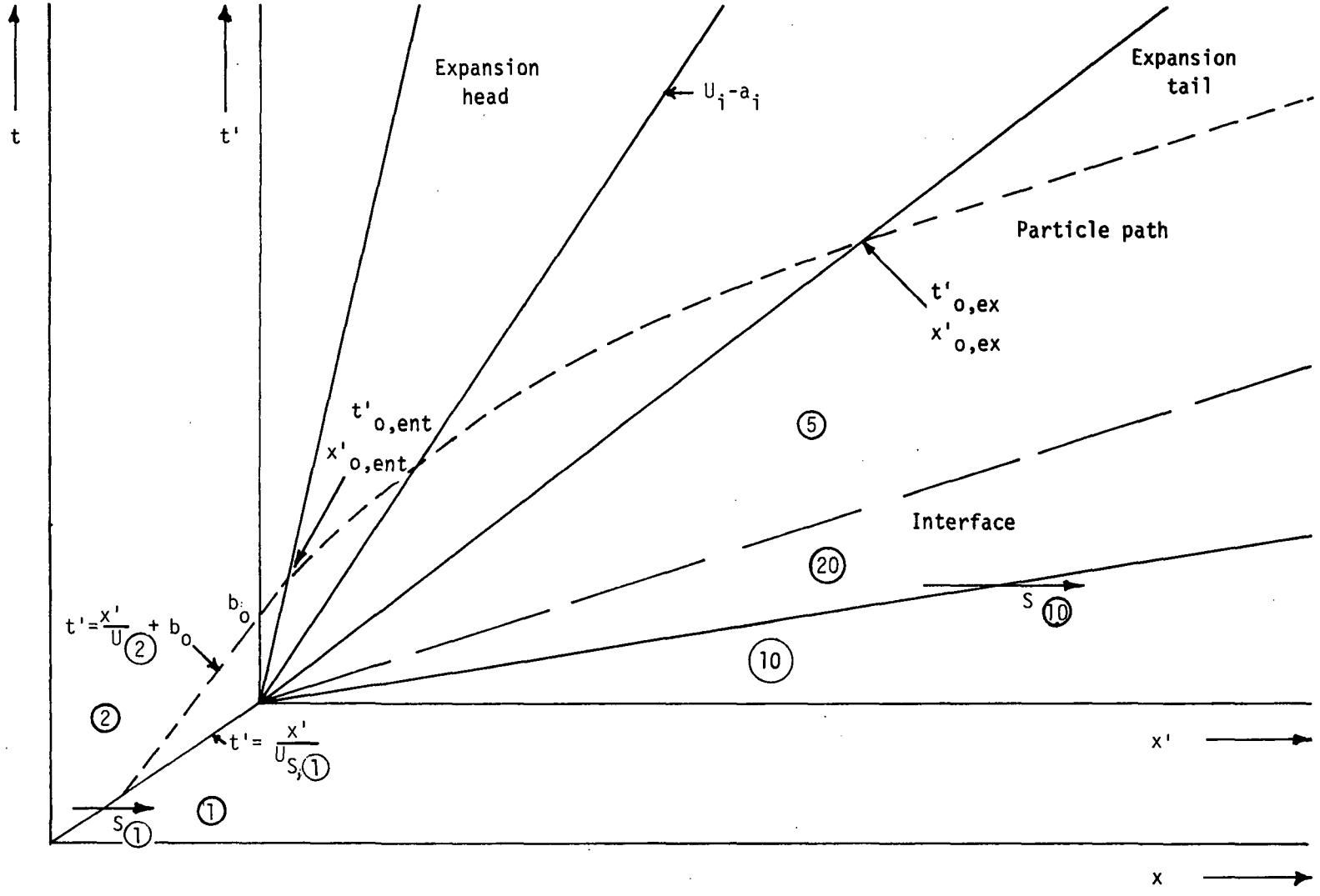


Figure 11.- Schematic used in the computation of the total integrated Reynolds number $R_t$.

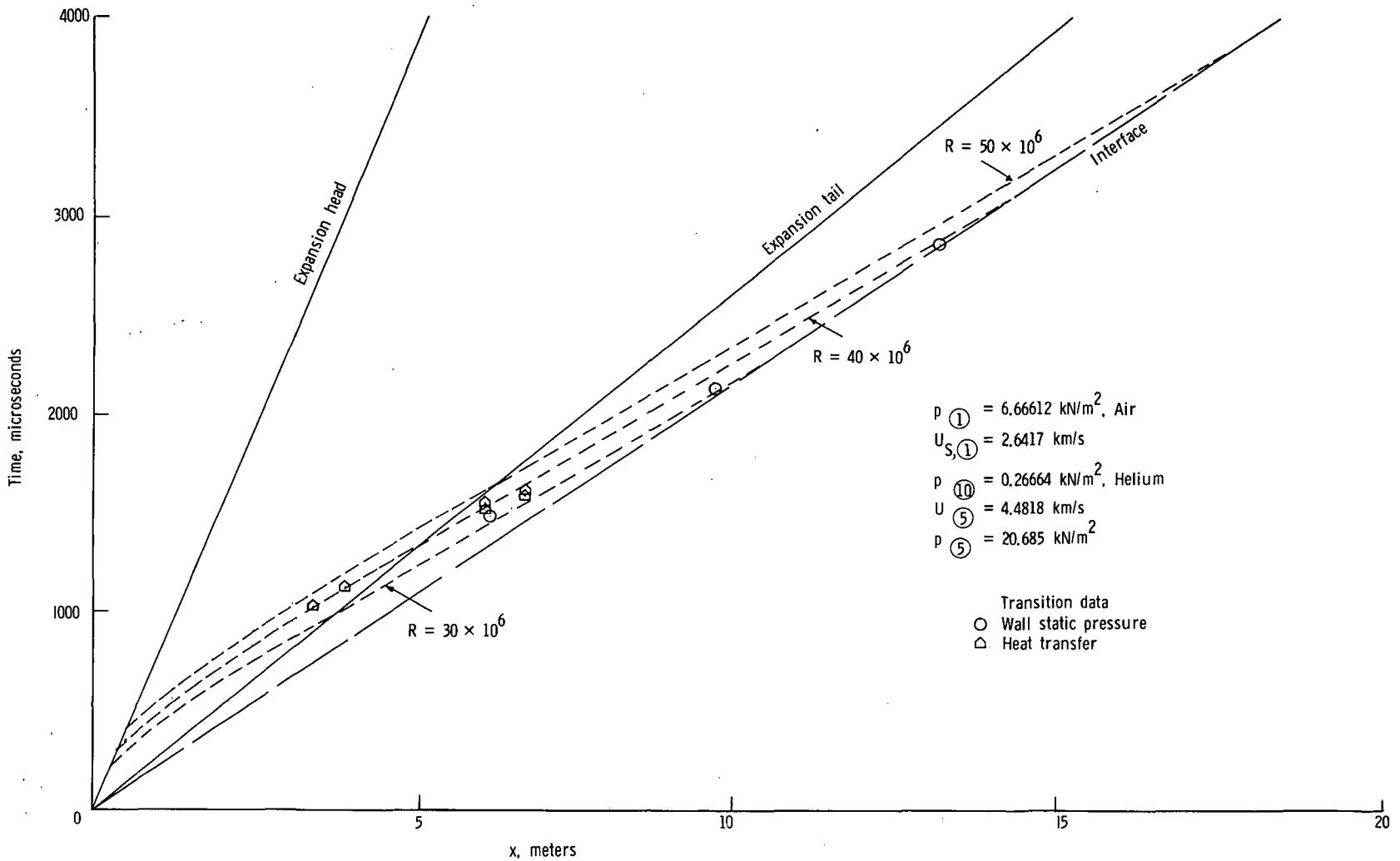


Figure 12.- Transition data as a function of integrated equilibrium Reynolds number.

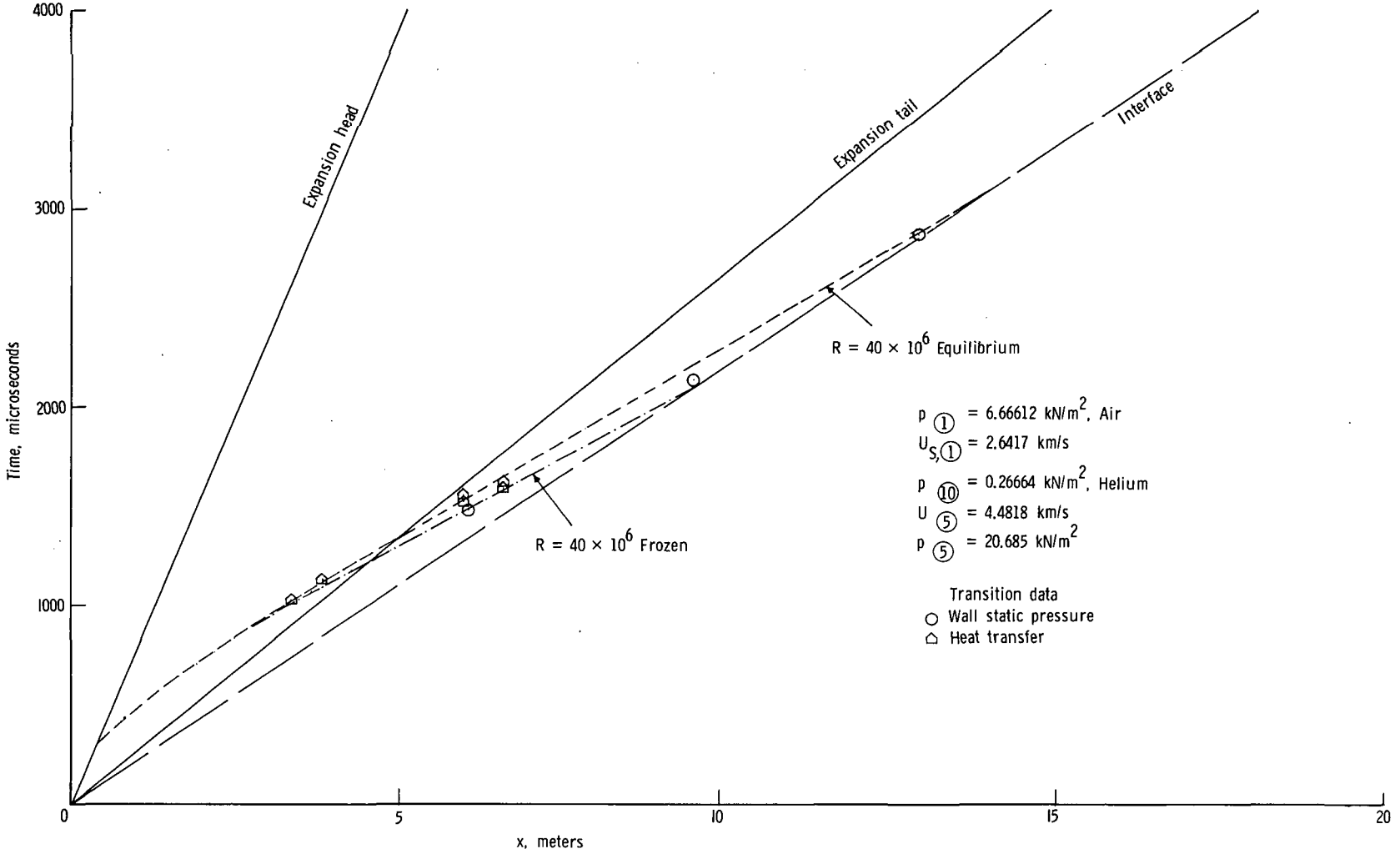


Figure 13.- Transition data as a function of integrated equilibrium and frozen Reynolds number.

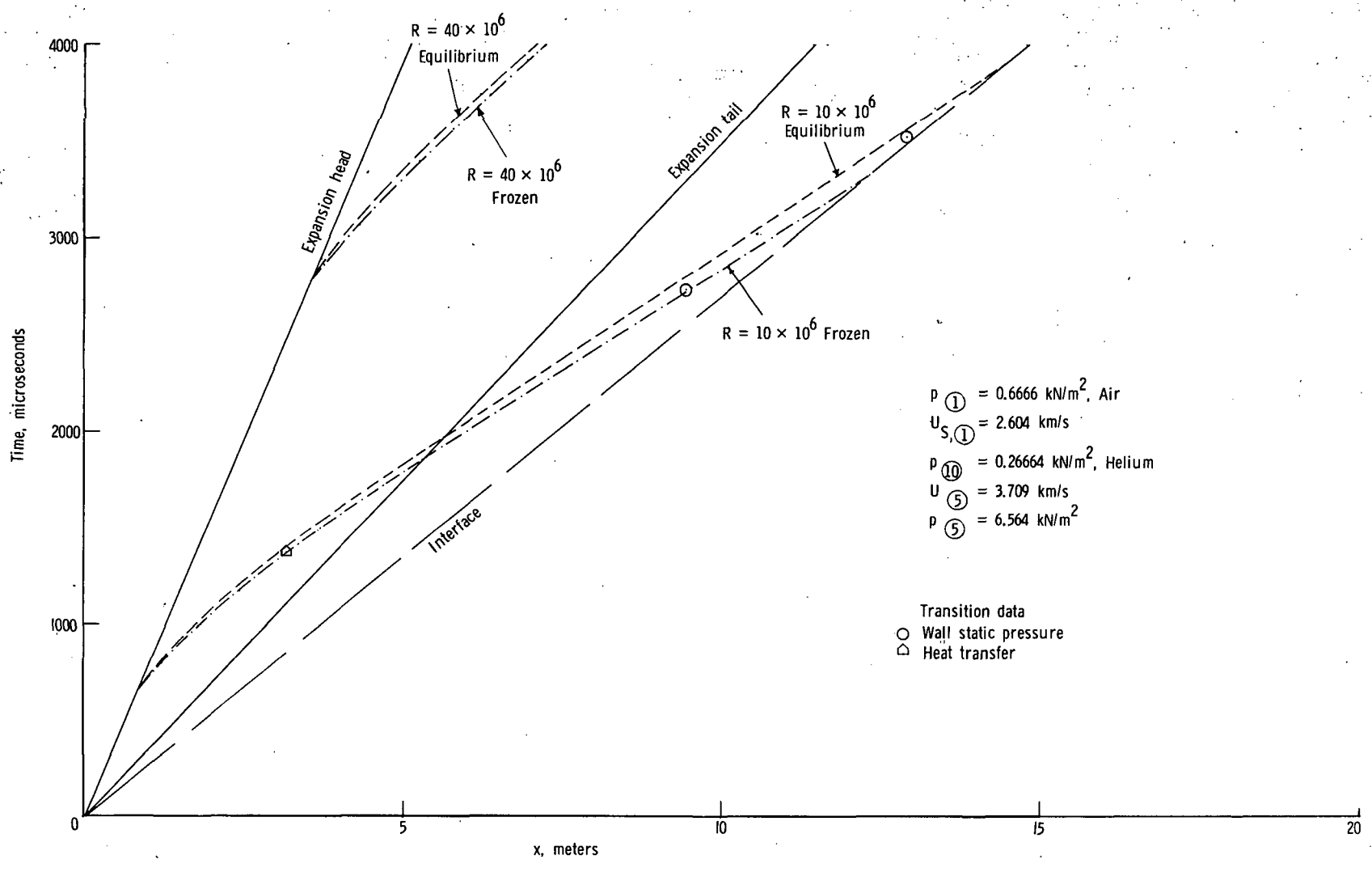


Figure 14.- Transition data as a function of integrated frozen and equilibrium Reynolds number. Near-frozen case.

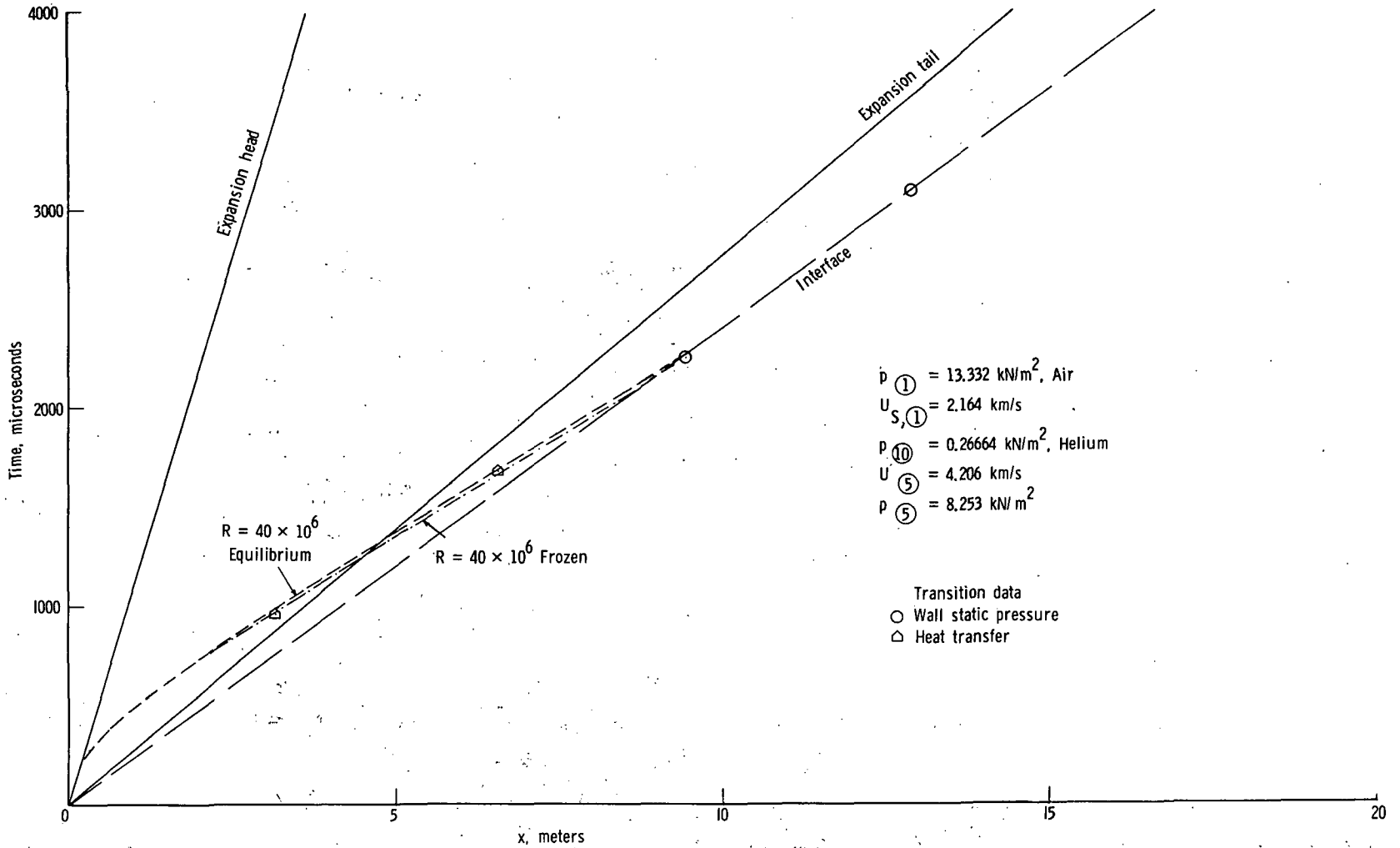


Figure 15.- Transition data as a function of integrated frozen and equilibrium Reynolds number. Near-equilibrium case.

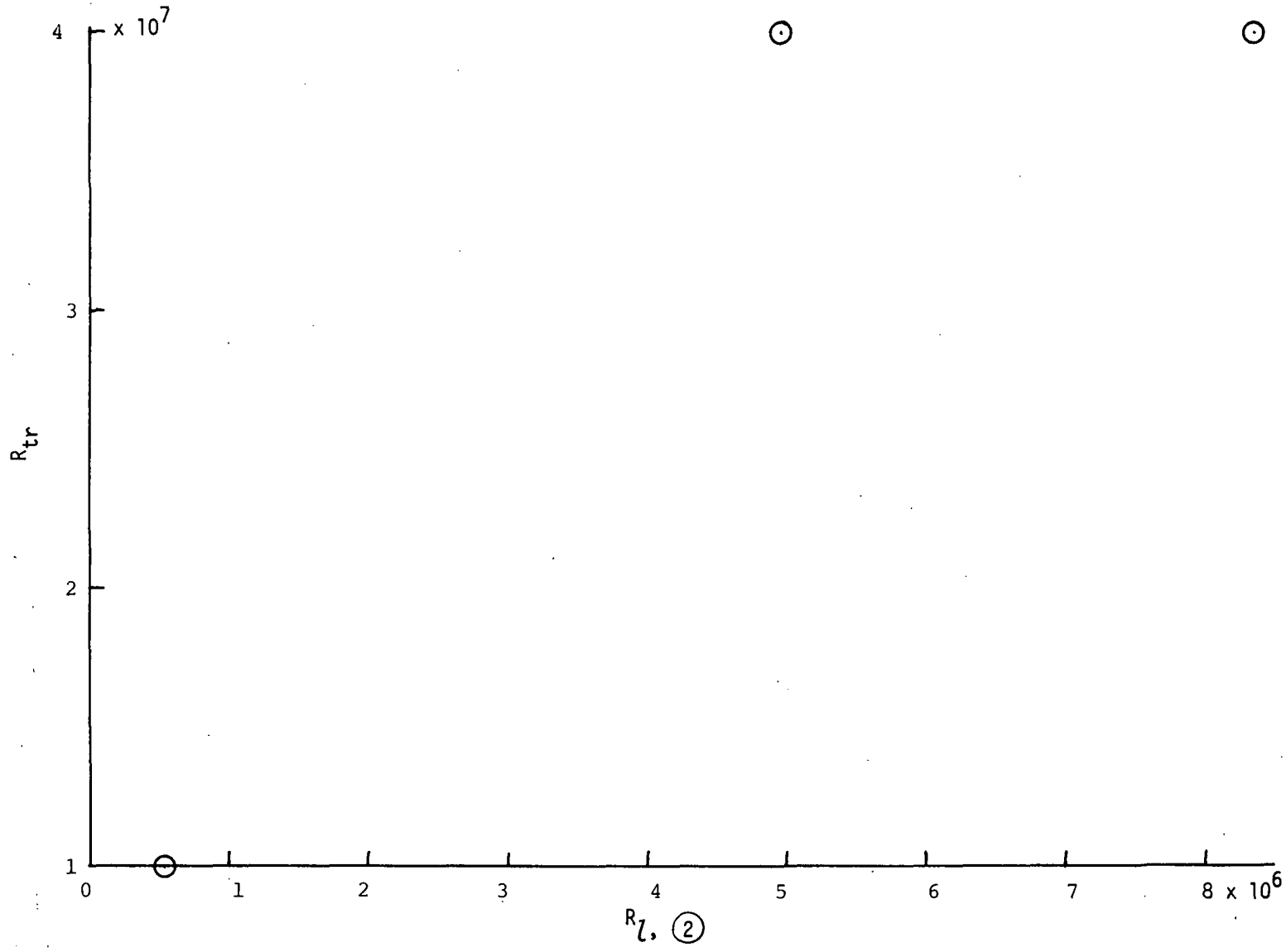


Figure 16.- Transition Reynolds number as a function of equilibrium unit Reynolds number in region $R_{l,②}$.

*"The aeronautical and space activities of the United States shall be conducted so as to contribute . . . to the expansion of human knowledge of phenomena in the atmosphere and space. The Administration shall provide for the widest practicable and appropriate dissemination of information concerning its activities and the results thereof."*

—NATIONAL AERONAUTICS AND SPACE ACT OF 1958

# NASA SCIENTIFIC AND TECHNICAL PUBLICATIONS

TECHNICAL REPORTS: Scientific and technical information considered important, complete, and a lasting contribution to existing knowledge.

TECHNICAL NOTES: Information less broad in scope but nevertheless of importance as a contribution to existing knowledge.

TECHNICAL MEMORANDUMS: Information receiving limited distribution because of preliminary data, security classification, or other reasons. Also includes conference proceedings with either limited or unlimited distribution.

CONTRACTOR REPORTS: Scientific and technical information generated under a NASA contract or grant and considered an important contribution to existing knowledge.

TECHNICAL TRANSLATIONS: Information published in a foreign language considered to merit NASA distribution in English.

SPECIAL PUBLICATIONS: Information derived from or of value to NASA activities. Publications include final reports of major projects, monographs, data compilations, handbooks, sourcebooks, and special bibliographies.

TECHNOLOGY UTILIZATION PUBLICATIONS: Information on technology used by NASA that may be of particular interest in commercial and other non-aerospace applications. Publications include Tech Briefs, Technology Utilization Reports and Technology Surveys.

***Details on the availability of these publications may be obtained from:***

**SCIENTIFIC AND TECHNICAL INFORMATION OFFICE**

**NATIONAL AERONAUTICS AND SPACE ADMINISTRATION**

**Washington, D.C. 20546**